Elevated levels of Ube2g1 in hematopoietic stem cells lead to segmental aging of the hematopoietic system

Julian Niemann,[1] Tanja Schuster,[1] Vadim Sakk,[1] Karin Soller,[1] Andreas Brown,[1] Sebastian Wiese,[2] Karina Eiwen,[1] Markus Hoenicka,[3] Andreas Liebold,[3] Moritz Oltmanns,[4] Heiko Reichel,[4] Medhanie A. Mulaw[5] and Hartmut Geiger[1]

[1]Institute of Molecular Medicine, Ulm University; [2]Core Unit Mass Spectrometry and Proteomics, Ulm University; [3]Department of Cardiothoracic and Vascular Surgery, University Hospital; [4]Department of Orthopaedic Surgery, University Hospital and [5]Single-Cell Sequencing Unit, Ulm University, Ulm, Germany

Correspondence: J. Niemann
julian.niemann@uni-ulm.de

H. Geiger
hartmut.geiger@uni-ulm.de

Received: July 31, 2025.
Accepted: January 23, 2026.
Early view: February 5, 2026.

https://doi.org/10.3324/haematol.2025.288847

©2026 Ferrata Storti Foundation
Published under a CC BY-NC license

Abstract

Aged hematopoietic stem cells (HSC) show diminished capacity of self-renewal, skewed lineage output and compromised proteostasis. Ubiquitin proteasomal systems are critical for maintaining protein homeostasis. We show that the levels of Ube2g1, a E2 ubiquitin-conjugating enzyme likely involved in clonal selection of HSC, was elevated in aged murine and human HSC. We hypothesized that elevated levels of Ube2g1 causally contribute to hematopoietic system aging. Elevated levels of Ube2g1 in young murine HSC resulted in increased myeloid-to-lymphoid ratio and reduced naïve T cells, both known hallmarks of hematopoietic aging. Interestingly, the ubiquitination function of Ube2g1 did not primarily account for the observed phenotypes. Elevated levels of Ube2g1 affected global tyrosine phosphorylation, mediated through a Ube2g1-Shp2 axis, which correlated with impaired T-cell development and reduced HSC function. Our work identifies a novel connection between proteins involved in the regulation of ubiquitination and phosphorylation in HSC that affect phenotypes linked to aging of HSC.

Introduction

Hematopoietic stem cells (HSC) are essential for maintaining a functional hematopoietic system throughout life. The delicate balance between self-renewal and differentiation is critical for preserving HSC function.[1,2] As organisms age, HSC undergo a functional decline, contributing to age-associated changes in the hematopoietic system.[3-5] The aging process in HSC involves a complex network of intra- and extracellular mechanisms, one of which is changes in proteostasis, the equilibrium between protein formation and degradation.[6,7] HSC maintain low protein synthesis rates and high translation accuracy, coupled with efficient protein degradation systems which are tightly regulated.[8,9]

Proteostasis comprises three main components: protein translation, folding, and degradation.[8,10] Previous research has emphasized the importance of protein translation and folding in quiescent cells like HSC.[8,11,12] But the nature of the degradation network within HSC has not been addressed in detail. A key player in protein degradation is the ubiquitin-proteasome system (UPS), which tags proteins with ubiquitin for subsequent degradation by the 26S proteasome.[4,7,13] During HSC aging, the efficiency of the UPS declines, leading to the accumulation of damaged and misfolded proteins in aggregates. The differential regulation of these aggregates between young and aged HSC affects HSC function.[14,15]

E2 enzymes mediate ubiquitin transfer between E1 activating enzymes and E3 ligases, contributing to the diversity of ubiquitination through target and E3 specificity.[16,17] Reported data support a role for the E2 ubiquitin-conjugating enzyme Ube2g1 in clonal selection of HSC upon aging. Ube2g1 is thought to primarily catalyse the addition of K48-linked ubiquitin chains, which typically signal for substrate degradation.[18] Ube2g1 has been further implicated in treatment resistance of multiple myeloma via self-establishment of K48-Ub chains, suggesting a complex role beyond supporting E3 ligases.[18,19] Recent studies demonstrated an involvement of Ube2g1 in TRAF7-mediated DBD degradation and a potential connection to 3'UTR shortening in T-cell development.[20,21]

Based on our preliminary data, we hypothesized that Ube2g1

is involved in HSC aging. We show here that increased levels of Ube2g1 in murine and human HSC confer segmental aging on young murine HSC and altered protein phosphorylation patterns, which correlated with changes in Shp2. Elevated levels of Ube2g1 impaired aging-associated T-cell development and reduced HSC function.

Methods

Mice

Young wild-type (WT) C57/BL6J mice (10-16 weeks, CD45.2$^+$) and aged RFP$^{ki/ki}$ mice (>80 weeks, CD45.2$^+$) were used for competitive transplantations. Isolated HSC were transduced and transplanted into lethally irradiated (7+4 Gy) young B6.SJL-Ptprc^a Pepc^b/BoyJ recipient mice (12-16 weeks, CD45.1$^+$). For other experiments young (10-16 weeks, CD45.2$^+$) and aged (>80 weeks, CD45.2$^+$) WT C57/BL6J mice were used.

Hematopoietic stem cell transduction

Long-term (LT)-HSC (Lin$^-$, c-Kit$^+$, Sca-1$^+$, CD34$^-$, Flt3$^-$) (*Online Supplementary Table S1*) were sorted from lineage depleted LDBM using FACS sorting (BD, Aria III). For transduction, HSC were incubated for 16 hours in mHSC medium (IMDM with 10% FBS, 1% Pen/Strep, 1% GlutaMAX, 100 ng/mL SCF, TPO and G-CSF) with viral particles (VP) at multiplicity of infection (MOI) of 30.

Flow cytometry

Spleen and thymus were forced through a 70 µm filter to retrieve single cells and red blood cells lysed (Biolegend) prior to flow analysis with an LSRFortessa (BD) (*Online Supplementary Table S1*).

Immunofluorescence

Young (median age: 32.5 years) and aged (median age: 71.0 years) human CD34$^+$ HSC were cultured in hHSC medium (StemSpan SFEM with 100 ng/mL SCF, 50 ng/mL TPO and 100 ng/mL (Fly3) (*Online Supplementary Table S2*). For preparation of cells for immunofluorescence (IF), we followed the protocol published by our group.[22] Antibodies are listed in *Online Supplementary Table S1*.

Proximity ligation assay

For proximity ligation assay (PLA) after fixation and permeabilization,[22] the Duolink Proximity Ligation Assay (Sigma-Aldrich) was used according to the manufacturer's instructions with the addition of GFP counterstaining.

Production and titration of lentiviral particles

Viral particles were generated using a Transfection Kit (Takara Bio). We used a GFP cassette that was inserted downstream of the ORF (Control, Ube2g1-OE, Dash between Ube2g1 and C90S = Ube2g1-C90S-OE, shScrambled and shUbe2g1) with a TRTRPLE linker. Plasmids were transfected in 293T-LentiX cells (TakaraBio) and VP harvested, concentrated by ultracentrifugation, and the titers determined.[23]

Mass spectrometry

Digestion, elution and measurement, as well as quantitative analysis and peptide identification with Andromeda, were performed as previously described.[24-26] To identify Ube2g1 interacting proteins, positive outliers found by Significance B testing[25] in addition to proteins with a log2 Ube2g1/ctrl ratio >2 were considered.

Ube2g1-OE^{C90S} generation

Data from Lu *et al.*[19] were used for the generation of the C90S mutated Ube2g1-OE plasmid. A site-directed mutagenesis kit (NEB) was used to introduce the base substitution (*Online Supplementary Figure S1A*).

RNA-sequencing

Transduced HSC were sorted and processed according to the SMART Seq. v4 Ultra Low Input RNA Kit (Takara Bio). Libraries were prepared with the Nextera XT library Kit (Illumina). Raw data were processed, aligned, and mapped as previously described.[27,28] For GoTerms analysis (*Online Supplementary Table S3*), differentially expressed genes (DEG) from selected comparisons were used in Gorilla.[29]

Ethical statement

Our research complies with all relevant ethical regulations and was performed in compliance with German Law for the Welfare of Laboratory Animals approved by the Regierungspräsidium Tübingen and the Ethikkommission of Ulm University (Institutional Review Board approvals: 66/24, 392/16).

Graphical illustrations

Graphical images were generated with BioRender.com under an Academic Lab License.

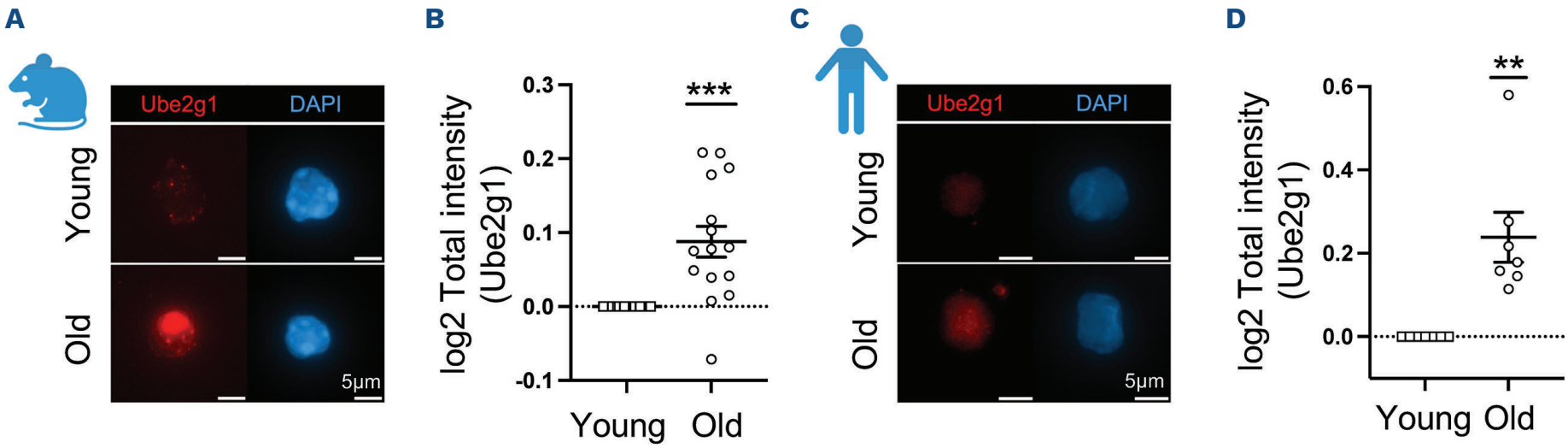
Quantification and statistical analysis

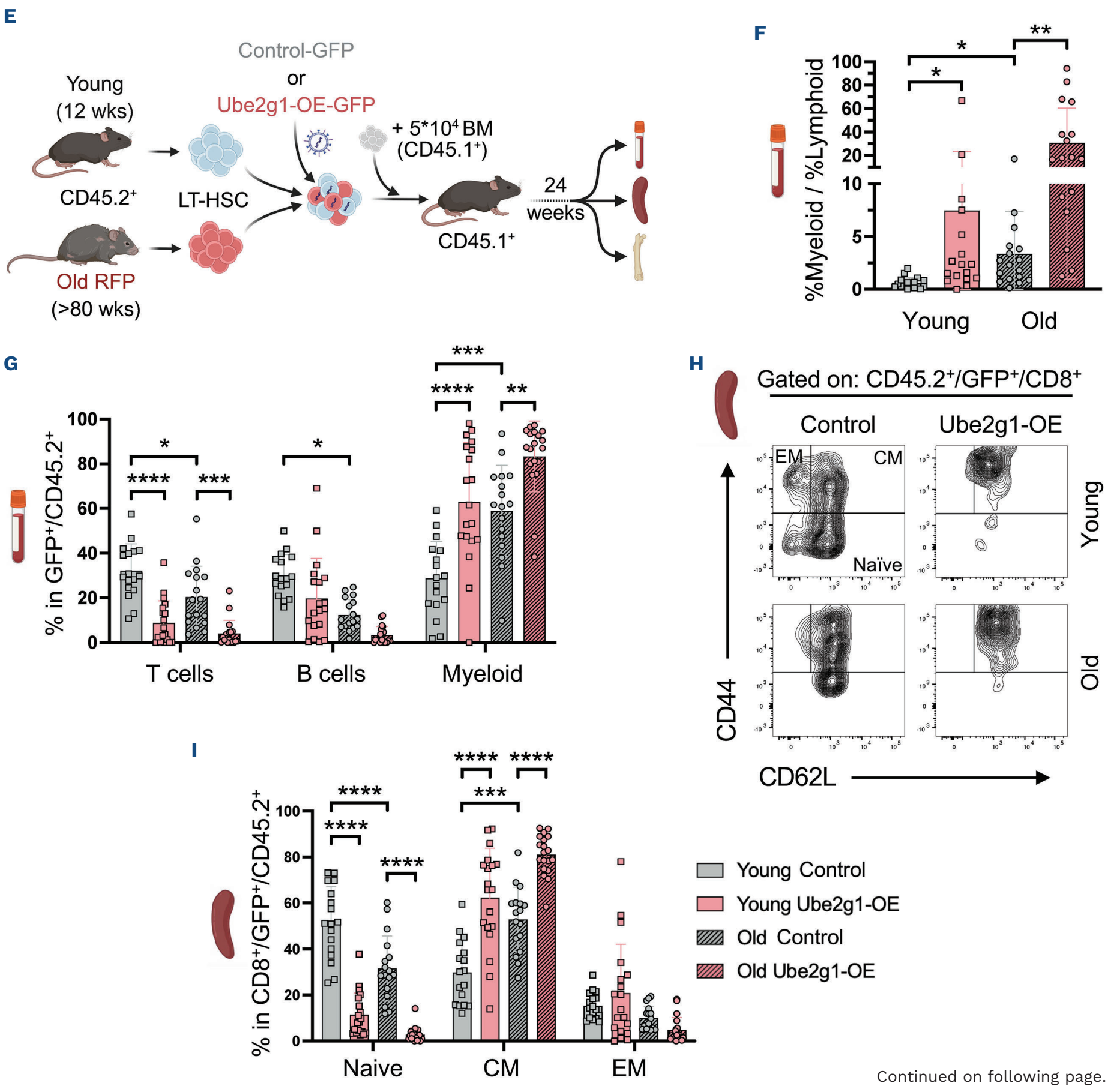
The statistical tests used are described in the respective figure legends. We performed multiple experiments with biological replicates to ensure data reproducibility.

Results

Expression of Ube2g1 is increased in aged murine hematopoietic stem cells and aged human hematopoietic stem and progenitor cells

A replication deficient retroviral insertional mutagenesis screen[30] identified, among others, elevated levels of Ube2g1, an E2 enzyme relevant for degradation specific K48-ubiquitination establishment, as a likely target for conferring aging-associated clonal advantages to HSC[22,31] (*Online Supplementary Figure S2A*). We, therefore, determined the level





Continued on following page.

Figure 1. Elevated levels of Ube2g1 result in segmental premature aging of hematopoietic stem cells. (A) Representative immunofluorescence (IF) images from young (12-16 weeks [wks] old, WT) and aged (>80 wks old, WT) murine hematopoietic stem cells (HSC) stained for Ube2g1 (red) and DAPI (blue). Scalebar = 5µm. (B) Relative (log2 transformed) intensity of Ube2g1 in young and old murine HSC (N=7-11, biological repeats equal to an average of 83/155 (young/old) cells per replicate). (C) Representative IF images of human CD34$^+$ hematopoietic stem and progenitor cells (HSPC) from young (25-33 years donors; mean = 30 years) and old (55-80 years; mean = 68 years) donors stained for Ube2g1 (red) and DAPI (blue). Scalebar = 5µm. (D) Relative (log2 transformed) intensity of Ube2g1 in young and old human CD34$^+$ HSPC (N=4-7, biological repeats equal to an average of 191/166 [young/old] cells per replicate). (E) Schematic of the experimental set-up of the competitive transplantation experiment, using sorted HSC from young (12-16 wks old, WT) and aged (>80 wks old, AcRFP$^+$) donor mice (CD45.2$^+$). HSC were genetically engineered and transplanted alongside 5 x10^4 CD45.1$^+$ bone marrow (BM) cells into lethally irradiated recipient mice (CD45.1$^+$). (F) Ratio of the percentage of donor-derived (GFP$^+$) myeloid (Gr-1$^+$/CD11$^+$) over lymphoid (CD3e$^+$, CD19$^+$) cells in peripheral blood (PB) 24 weeks post transplantation (N=16-19; 4 independent experiment repeats). (G) Percentage of donor-derived (GFP$^+$) T cells (CD3e$^+$), B cells (CD19$^+$) and myeloid cells (Gr-1$^+$/CD11$^+$) in PB 24 weeks post transplantation (N=17-19; 4 independent experiment repeats). (H) Representative flow cytometry plots showing splenocytes gated for young and aged naïve (CD62L^{dim}, CD44$^-$), effector (EM; CD62L$^-$, CD44$^+$), and central memory cells (CM; CD62L$^+$, CD44$^+$) in animals transplanted with HSC transduced with Ube2g1-OE or control virus. (I) Percentage of donor-derived (GFP$^+$) naïve, CM and EM CD8$^+$ T cells in the spleen 24 weeks post transplantation (N=17-19; 4 independent experiment repeats). Data show individual biological replicates with each replicate as mean ± standard error of mean (SEM) (B, D) or mean ± standard deviation (SD) (F, G, I) from 4 independent repeats for mouse experiments. Data were assessed by a One sample *t* test against a value of 0 for young control (B, D) or by One-Way ANOVA or Kruskal-Wallis test depending on normality (F, G, I). **P*<0.05, ***P*<0.01, ****P*<0.001, *****P*<0.0001.

of Ube2g1 protein in young and aged murine HSC by quantitative immunofluorescence imaging (QIF[22]). Aged murine LT-HSC (Lin$^-$, Sca1$^+$, c-Kit$^+$, CD34$^-$, Flt3$^-$) exhibited increased levels of Ube2g1 protein compared to young cells (Figure 1A, B). Levels of ubiquitin and lysine-48-linked ubiquitin (K48-Ub), proteins that are, like Ube2g1, critical for protein degradation, showed a mild reduction in the case of overall ubiquitin (*Online Supplementary Figure S2B, C*), while there was an increase in the level of K48-Ub (*Online Supplementary Figure S2D, E*). K48-Ub primarily targets proteins towards proteasomal degradation. Elevated levels of K48-Ub have also been reported in age-related protein aggregation diseases.[32-34] Similarly to our findings in murine HSC, the levels of both Ube2g1 and K48-Ub were also increased in aged human bone marrow (BM)-derived CD34$^+$ HSPC (donor >60 years) compared to HSC from young donors <30 years, while levels of ubiquitin were not affected by aging (Figure 1C, D, *Online Supplementary Figure S2F-I*). These findings are consistent with elevated levels of proteins marked for degradation in aged HSC, while further experiments will be required to test for the overall flux of protein degradation in especially aged human HSC.

Elevated levels of Ube2g1 result in segmental premature aging of hematopoietic stem cells

We next investigated the extent to which an elevated level of expression of Ube2g1 in young HSC changes functional parameters in HSC that are associated with aging. Competitive transplantation experiments of young and aged LT-HSC transduced with a GFP-tagged Ube2g1 that conferred elevated levels of expression of Ube2g1 to HSC (overexpression [OE] HSC) (Figure 1E, *Online Supplementary Figure S3A-D*) revealed a pronounced myeloid bias (myeloid cell frequency over lymphoid cell frequency) driven by OE HSC in peripheral blood (PB) of the recipient mice. There was a 3-fold increase of the myeloid bias in animals transplanted with OE young cells, which increased to 18-fold in recipients of OE aged HSC when compared to the myeloid over lymphoid ratio in animals transplanted with HSC transduced with a control virus (Figure 1F). The shift was due to a 4-fold decrease in T cells and a 2-fold increase in myeloid cells in recipients of young OE HSC, while animals transplanted with aged OE cells showed a 6-fold reduction in T cells and a 50% increase in myeloid cells in the PB compared to controls (Figure 1G). This myeloid shift was also present in the spleen, but not in the BM of the recipients (*Online Supplementary Figure S3E-H*). Elevated levels of OE did not affect the frequency of young HSC or the aging-associated increase in aged HSC,[3,35] or the frequency of young and aged myeloid progenitor cells in BM (*Online Supplementary Figure S3 I, J*).

Upon aging, there is a reduction in the frequency of naïve CD8$^+$ T cells and an increase in the frequency of CD8$^+$ memory T cells in spleen.[28,36] Recipients of young OE HSC already showed a substantial reduction in the frequency in naïve CD8-positive T cells (CD8$^+$, CD44$^-$, CD62L$^+$) (Figure 1H, I), while they were completely absent in recipients of aged OE HSC. Conversely, the frequency of central memory T cells (CD8$^+$, CD44$^+$, CD62L$^+$) was increased in the spleen of recipients that received either young or aged OE HSC. The frequency of effector T cells (CD8$^+$, CD44$^+$, CD62L$^-$) was not affected in OE-transplanted mice. Moreover, also the frequency of naïve (lower upon aging) and memory (elevated upon aging) CD4$^+$ T cells in the spleen of animals transplanted with Ube2g1-OE HSC mirrored the frequency of their CD8$^+$ counterparts in OE HSC recipients (*Online Supplementary Figure S3K*). Collectively, these findings support the view that elevated levels of Ube2g1 in HSC can be causative for segmental aging-like differentiation phenotypes of HSC.

We next investigated the extent to which a reduction in the expression of Ube2g1 in aged HSC might reduce aging-associated phenotypes of aged HSC. Competitive transplantation

experiments of aged LT-HSC transduced with an GFP-tagged shRNA against Ube2g1 that reduced elevated levels of expression in aged HSC (KD HSC) (*Online Supplementary Figure S4A-D*) demonstrated that, indeed, reduced levels of Ube2g1 resulted in a decreased myeloid bias compared to aged controls (*Online Supplementary Figure S4E, F*), driven by a lower frequency of myeloid cells in combination with a modest increase in T and B cells in PB. Ube2g1-KD in aged HSC did not affect the aging-associated reduction in naïve $CD8^+$ T cells in spleen or myeloid bias reported for aged HSC (*Online Supplementary Figure S4G, H*). T, B, and myeloid cells in BM were similar to animals transplanted with aged control HSC (*Online Supplementary Figure S4 I*), while the aging-associated increase in the frequency of HSC in aged BM was reduced in animals transplanted with aged Ube2g1-KD HSC (*Online Supplementary Figure S4J*). While these data support an overall causal role of an elevated level of Ube2g1 for conferring aging-associated phenotypes on HSC, they also reveal that there is only a segmental set of phenotypes affected by Ube2g1.

The ubiquitination function of Ube2g1 is not required for conferring aging-associated phenotypes on hematopoietic stem cells

Lu *et al.* demonstrated, in large sets of experiments, that a C90S point mutation in Ube2g1 renders the ubiquitination function of Ube2g1 inactive, and that Ube2g1-C90S is not able to ubiquitinate target proteins.[19] We, therefore, performed competitive transplantation experiments with HSC that were transduced with Ube2g1-C90S-OE to test for the role of the ubiquitination function of Ube2g1 for conferring the aging-associated phenotypes (Figure 2A, B, *Online Supplementary Figure S1A-D*). Unexpectedly, Ube2g1-C90S-OE did not alter the segmental aging phenotype conferred by the elevated level of Ube2g1. Recipients receiving Ube2g1-C90S-OE HSC still exhibited a 12-fold increase in the myeloid-to-lymphoid cell ratio in PB due to a reduction in T cells and an increase in myeloid cells (Figure 2C, D). Also, the reduction in frequency of naïve $CD8^+$ T cells and an increase in the frequency of effector T cell (Figure 2E), as well as a shift in the myeloid-to-lymphoid ratio in the spleen (*Online Supplementary Figure S1E, F*) conferred by Ube2g1-OE was not affected by the point mutation. Ube2g1-C90S HSC mirrored the function of Ube2g1-OE HSC also with respect to the frequency of mature T, B, and myeloid cells, as well as LT-HSC and myeloid progenitor populations in BM (*Online Supplementary Figure S1G-I*). Collectively, these findings imply that enzymatic function - “ubiquitination of target substrates bound to an E3 enzyme” - of Ube2g1 is probably not the main mechanistic driver conferring aging-like phenotypes on Ube2g1-OE HSC.

Elevated levels of Ube2g1 result in changes in phosphorylation and immune system pathways

We next employed RNA sequencing approaches on Ube2g1-OE HSC to obtain insights into likely molecular mechanisms on the action of Ube2g1 (Figure 3A). Analysis of the sample distribution using a 2-dimensional PCA identified a greater heterogeneity among young Ube2g1-OE HSC compared to aged Ube2g1-OE HSC (Figure 3B). While there was an overall large number of DEG between young and aged cells, unsupervised clustering of differentially expressed genes revealed a strong shift in the transcriptional landscape of young Ube2g1-OE hematopoietic stem and progenitor cells (HSPC), while a more muted difference was observed for the transcriptional pattern of aged Ube2g1-OE HSPC (Figure 3C). Clustering of the DEG into functional groups via Gene Ontology (GO) analyses revealed terms associated with protein phosphorylation among the top hits, along with terms related to cytokine production (Figure 3D, *Online Supplementary Table S3*). So far, Ube2g1 has not been associated with a role in the regulation of protein phosphorylation. To obtain additional information with respect to the phosphorylation-related terms, these DEG were plotted on a volcano plot. Additional analyses revealed a strong association of GO in Ube2g1-OE HSPC with TCR and MAPK signaling, represented by Zap70 and Ptpn11 (Shp2) expression (Figure 3E, *Online Supplementary Table S4*).

In parallel co-immunoprecipitation (Co-IP) and mass spectrometry approaches, we identified potential protein interaction partners of Ube2g1 (Figure 3F, G, *Online Supplementary Table S5*). We identified Uba52, an E1 ubiquitin donor, as a likely prime Ube2g1-OE partner (*Online Supplementary Figure S5A, B*). Unexpectedly, Shp2 (a phosphatase), for which we observed increased expression in young Ube2g1-OE compared to control HSC, emerged again as a potential interactor. Furthermore, we identified a cluster of heat shock proteins (Hspa1a, Hspa2, Hspa4, Hspa8) as potential binding partners. We, therefore, also investigated a likely role of heat shock factor 1 (Hsf1), a regulator of heat shock protein expression, in Ube2g1-OE HSC. Young Ube2g1-OE HSC showed reduced levels of Hsf1, which aligns with an age-associated decrease in Hsf1 expression in HSPC (*Online Supplementary Figure S5C, D*). We made use of PLA to confirm key interactors of Ube2g1 in HSC. In physiological control conditions, we found Ube2g1 to be in close proximity (less than 40 nm) to both Creb3, a leucine zipper DNA binding protein, and Uba52. The average frequency of such a very close interaction of Ube2g1 with either Creb3 or Uba52 was increased in Ube2g1-OE HSC, suggesting increased levels of interaction upon an increase in protein (*Online Supplementary Figure S5E-K*), further supporting direct interaction of these proteins.

Elevated levels of Ube2g1 reduce global tyrosine phosphorylation and the level of Shp2 phosphatase

As the RNA-sequencing as well as the Co-IP analyses showed changes in general protein phosphorylation in response to elevated levels of Ube2g1 in HSC, we determined

the level of protein phosphorylation as well as the level of Shp2 expression in Ube2g1-OE HSC (Figure 4A, *Online Supplementary Figure S6A*). In aged HSC, the level of tyrosine-specific phosphorylation (pTyr) was decreased to 60% compared to young HSC. Ube2g1-OE in young HSC reduced the level of pTyr to that of aged HSC (Figure 4B, C). Interestingly, there was a high level of correlation for the localization of pTyr and Ube2g1 within HSC, with Pearson correlation co-efficients (PCC) of approximately 0.7 across all samples (Figure 4D).

In contrast to increased expression of Shp2 in our transcriptomic data, we observed a reduction in Shp2 protein levels in young Ube2g1-OE HSC (Figure 4E, F). Mirroring Ube2g1 and pTyr, the level of co-localization (PCC) between Ube2g1 and Shp2 was high across all samples, suggesting an elevated likelihood of protein interactions (Figure 4G). We also determined the level of pTyr and Shp2 in Ube2g1-KD and Ube2g1-C90S-OE in comparison to their respective

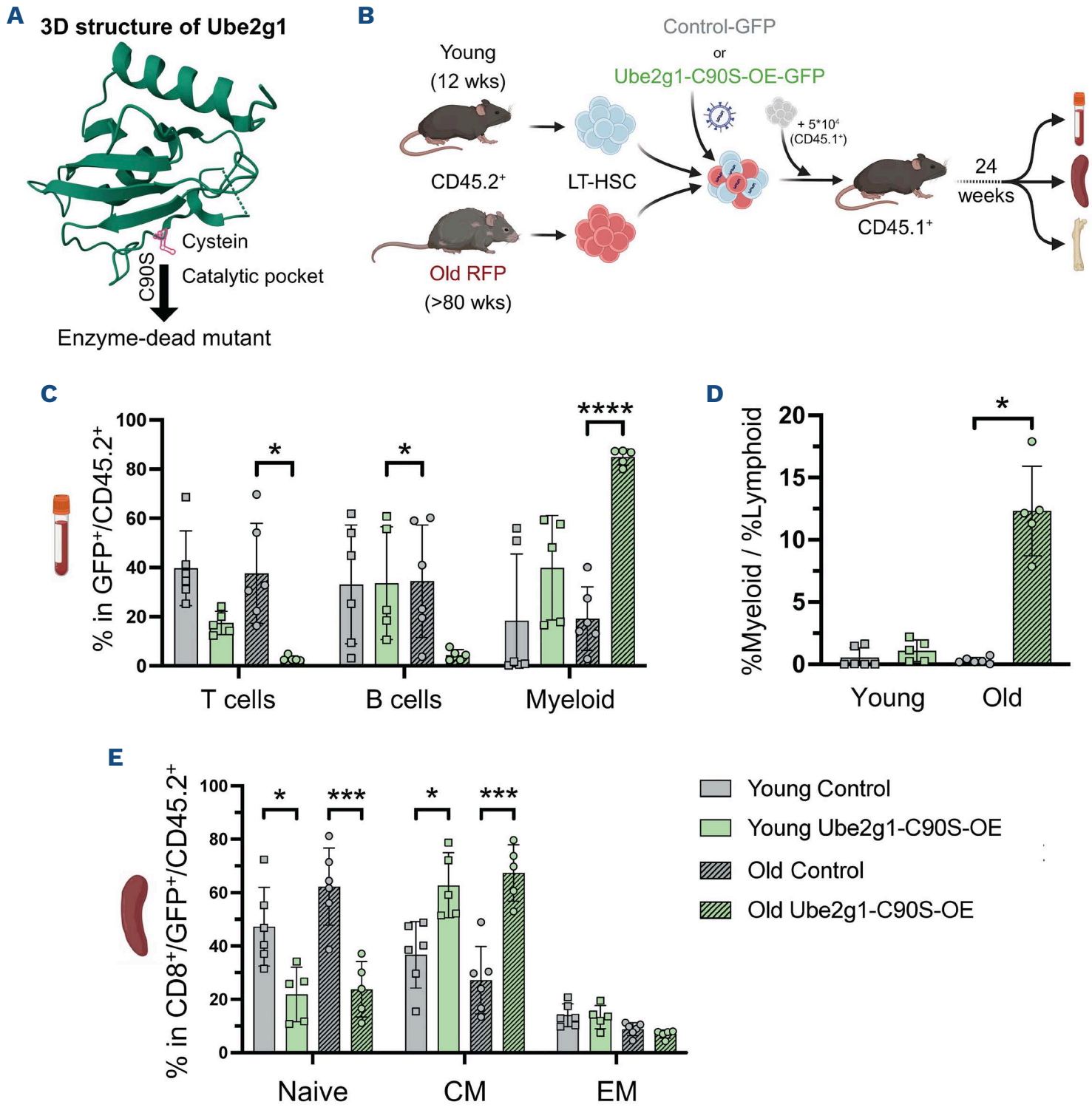
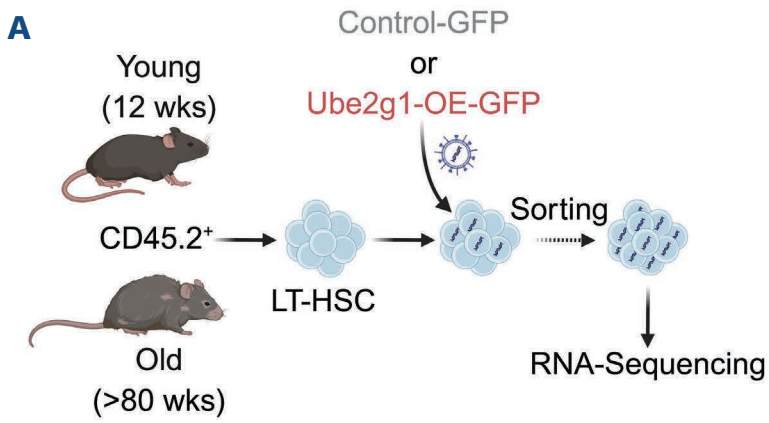
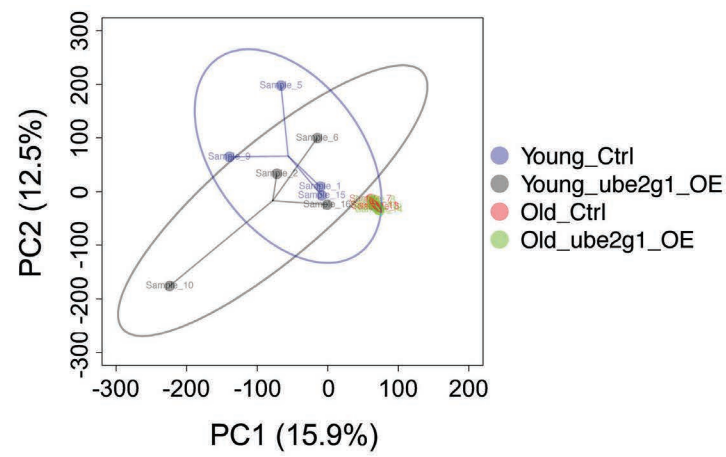
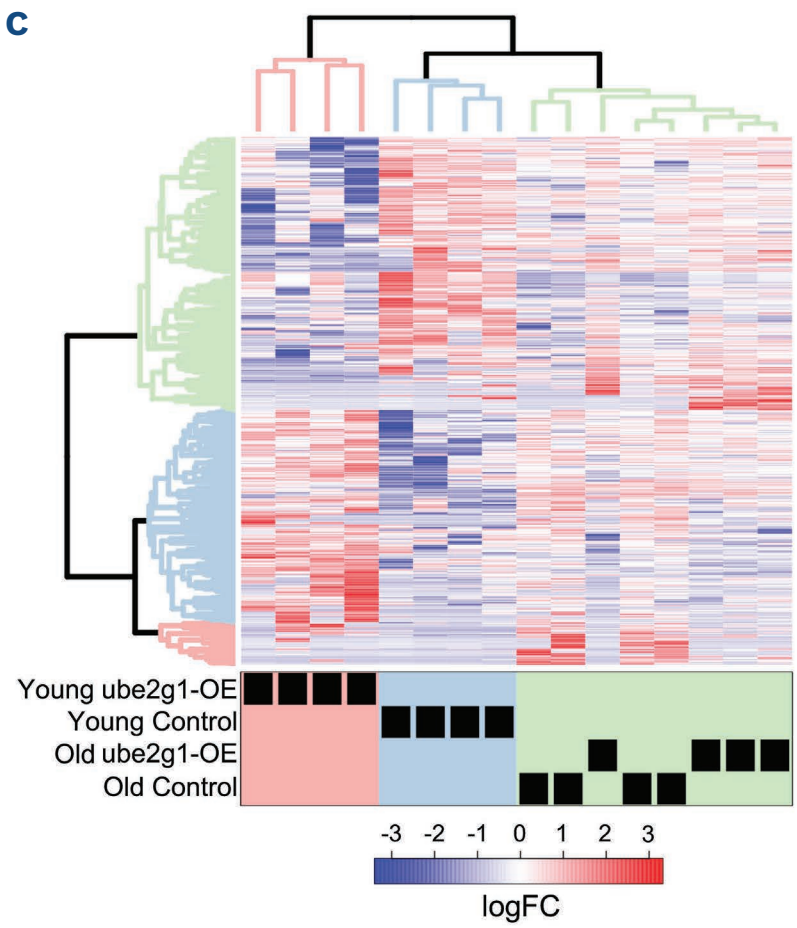
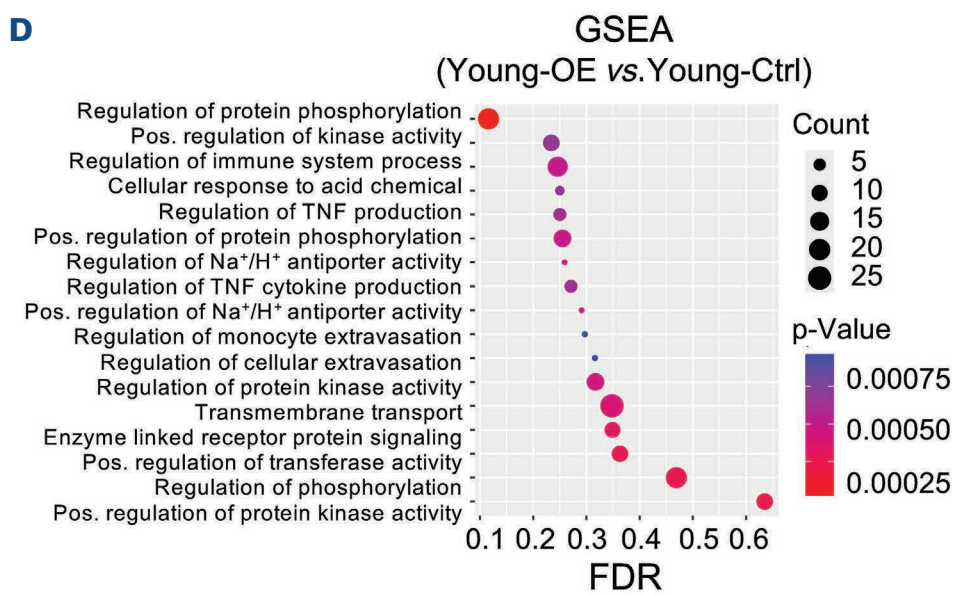


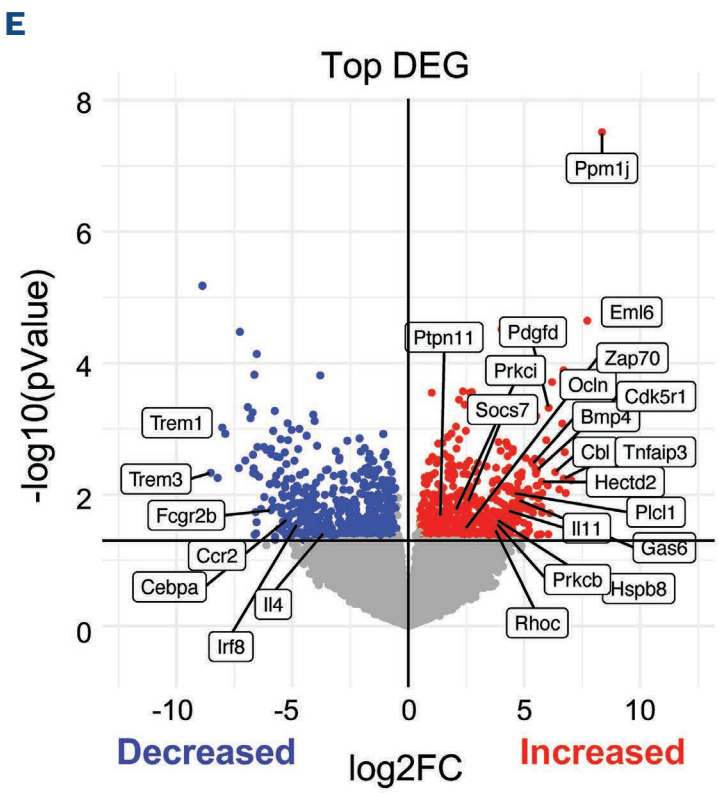
Figure 2. The ubiquitination function of Ube2g1 is not required for conferring aging-associated phenotypes on hematopoietic stem cells. (A) Schematic of the 3D structure of Ube2g1 with cysteine at position 90 highlighted within the active site of the enzyme. The substitution of cysteine with serine (C90S) in the active pocket leads to enzymatic inhibition of the UBC domain. (B) Schematic of the experimental set-up of the competitive transplantation experiment, using sorted hematopoietic stem cells (HSC) from young (12-16 weeks [wks], wild-type [WT]) and aged (>80 wks, AcRFP$^+$) donor mice (CD45.2$^+$). HSC were genetically engineered and transplanted alongside 5 x10^4 CD45.1$^+$ bone marrow (BM) cells into lethally irradiated recipient mice (CD45.1$^+$). (C) Percentage of donor-derived (GFP$^+$) T (CD3e$^+$), B (CD19$^+$), and myeloid (Gr-1$^+$/CD11$^+$) cells in peripheral blood (PB) 24 weeks post transplantation (N=5-6). (D) Ratio of percentage of donor-derived (GFP$^+$) myeloid over lymphoid cells in PB 24 weeks post transplantation (N=5-6). (E) Percentage of donor-derived (GFP$^+$) naïve, central memory (CM) and effector memory (EM) CD8$^+$ T cells in the spleen 24 weeks post transplantation (N=5-6). Data show individual biological replicates as mean ± standard deviation (SD). Data were assessed by One-Way ANOVA or Kruskal-Wallis test depending on normality (C-E). *P<0.05, ***P<0.001, ****P<0.0001.

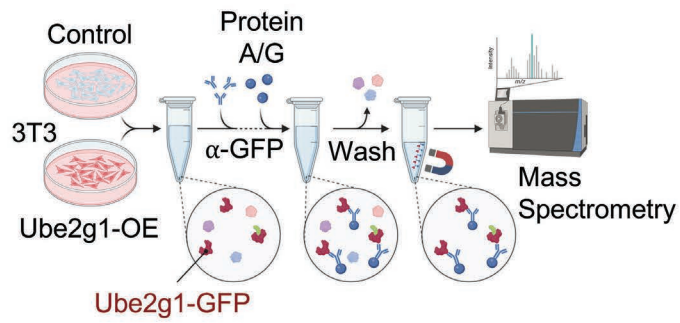


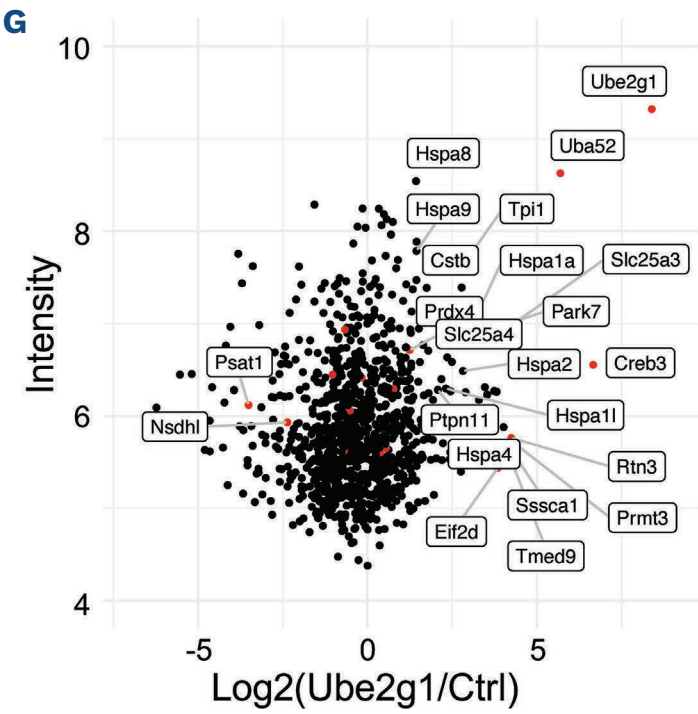












Continued on following page.

Figure 3. Elevated levels of Ube2g1 result in changes in phosphorylation and immune system pathways. (A) Schematic of the workflow for RNA-Sequencing sample preparation. Hematopoietic stem cells (HSC) from young (12-16 weeks [wks], wild-type [WT]) and aged (>80 wks, WT) mice were genetically engineered and then sorted for GFP$^+$. The resulting cells were used for library preparation prior to RNA-sequencing. (B) Principal component analysis (PCA) (N=4 biological replicates per condition). (C) Heatmap comparing young and old control (Ctrl) or Ube2g1-OE for differentially expressed genes (DEG) between groups. Rows represent fold-change between different conditions and columns individual samples. Samples are subclustered according to similarities as depicted on the bottom of the heatmap and indicated as colors and black bars. (Left) Gene clusters according to subclusters from the DEG analysis. (Top) Phylogenetic tree for sample similarity depending on DEG. (D) Gene set enrichment analysis (GSEA) for the comparison of DEG between the young samples with OE and Ctrl. All resulting gene ontologies (GO) are depicted. Color indicates *P* value and size of the circle gene counts. FDR: false discovery rate. (E) Comparison of significant DEG between young OE and Ctrl. (Top) Genes associated with the terms found in the GSEA are highlighted. (F) Workflow for immunoprecipitation (IP) followed by mass spectrometry for NIH/3T3 cells stably transduced with control or Ube2g1-OE. (G) Proteins found in the comparison between NIH/3T3 cells with Ube2g1-OE and control after IP. (See also Online Supplementary Table S5). Proteins that show significant differential presence are highlighted as red dots.

control. There was an overall reduced level for both pTyr and Shp2, and their levels were similar to those observed in Ube2g1-OE and aged HSC (*Online Supplementary Figure S6B-E*). Inhibition of Shp2 by a specific pharmacological inhibitor (SHP099) resulted, as anticipated, in reduced levels of the active form of Shp2 (phosphorylated at tyrosine 542, Figure 4H) and in the subsequently elevated levels of pTyr in HSC (Figure 4 I). Interestingly, inhibition of Shp2 in Ube2g1-OE HSC, while further reducing the level of Shp2-pY452, did not affect the level of pTyr in HSC. To test for a direct (less than 40 nm) Ube2g1-Shp2 interaction, PLA were performed. Ube2g1 interacts with Shp2 in young and old control HSC. The average interactions per cell did increase 2-fold in Ube2g1-OE HSC. These data further confirmed results from our mass spectrometry and RNA-sequencing analyses (Figure 4J-L). In summary, the data support that elevated levels of Ube2g1 reduce the amount of pTyr in HSC, while they also reduce levels of Shp2 and that Ube2g1 can directly interact with Shp2. Overall, the data thus suggest a complex relationship between Ube2g1, Shp2 and levels of pTyr in HSC, which might be explained by a model in which Ube2g1 serves as a protein interaction platform to balance active forms of proteins involved in the regulation of overall protein phosphorylation.

Elevated levels of Ube2g1 result in attenuated T-cell development in the thymus and increased exhaustion in released peripheral T cells

Shp2 and protein phosphorylation are, among others, known regulators of T-cell development, and Ube2g1-OE in HSC strongly affected the level of mature T cells in the periphery (Figure 1G). Ube2g1 might, therefore, affect also thymic T-cell development (Figure 5A). T-cell development in the thymus involves three key stages: double-negative (DN1$^-$DN4; CD4$^-$CD8$^-$), double-positive (DP; CD4$^+$CD8$^+$), and single-positive (SP; CD4$^+$ or CD8$^+$, CD3$^+$) cells (Figure 5B). In concordance with a general age-related increase in frequency, the percentage of DP thymocytes was also significantly increased in mice transplanted with young OE HSC. The data further suggested a partial impairment in the DP-to-SP transition and an accelerated DN1-to-DN2 progression, with an additional potential blockage of OE cells in DN2 and DN3 (Figure 5C-E). Elevated levels of Ube2g1, therefore, likely affect multiple transition points in thymic T-cell development. In addition to the relative changes within the populations, we observed a reduction in each cell type analyzed in recipients of young OE HSC, along with a reduction in cell populations in recipients transplanted with aged control HSC (*Online Supplementary Figure S7A, B*). To investigate additional changes in maturation of T cells downstream of the thymus, we also assessed the level of exhaustion of T cells (expression of Tim-3 and PD-1) (Figure 5F). Recipients of Ube2g1-OE HSC exhibited an elevated frequency of CD8$^+$ Tim-3$^+$ positive cells and a marked enrichment of Tim-3$^+$/PD-1$^+$ double-positive cells in spleen, similar to cells from spleen from aged mice, which implies increased levels of T-cell exhaustion. However, the frequency of PD-1$^+$ T cells, although elevated in aged HSC, was not affected by Ube2g1-OE (Figure 5G). Exhaustion in CD4$^+$ T cells mirrored the level of exhaustion seen in CD8$^+$ splenocytes (*Online Supplementary Figure S7C*). To investigate the extent of Shp2 involvement in this T-cell deficiency, *in vitro* CD8 T-cell activation/proliferation assay (activation by anti-CD3/CD28) were performed (*Online Supplementary Figure S7D*). CD8$^+$ Ube2g1-OE T cells showed a lower extent of activation in the activation/ expansion assays when compared to control T cells (*Online Supplementary Figure S7E-G*). There were reduced levels of active Shp2 (Shp2-pY542) in Ube2g1-OE T cells, accompanied by increased levels of pTyr in both young Ube2g1-OE and old control T cells (*Online Supplementary Figure S7H, I*). Ube2g1, therefore, affects T cells at multiple steps along their differentiation, maturation, activation and exhaustion trajectory. This implies a more general role for Ube2g1 in T-cell differentiation and function, which is consistent with a role of Ube2g1 in regulating more general patterns of phosphorylation.

Discussion

Several E2 conjugation enzymes, which mediate the transfer of ubiquitin to substrates bound to E3 ligases which then mark proteins for degradation, have been shown to play a

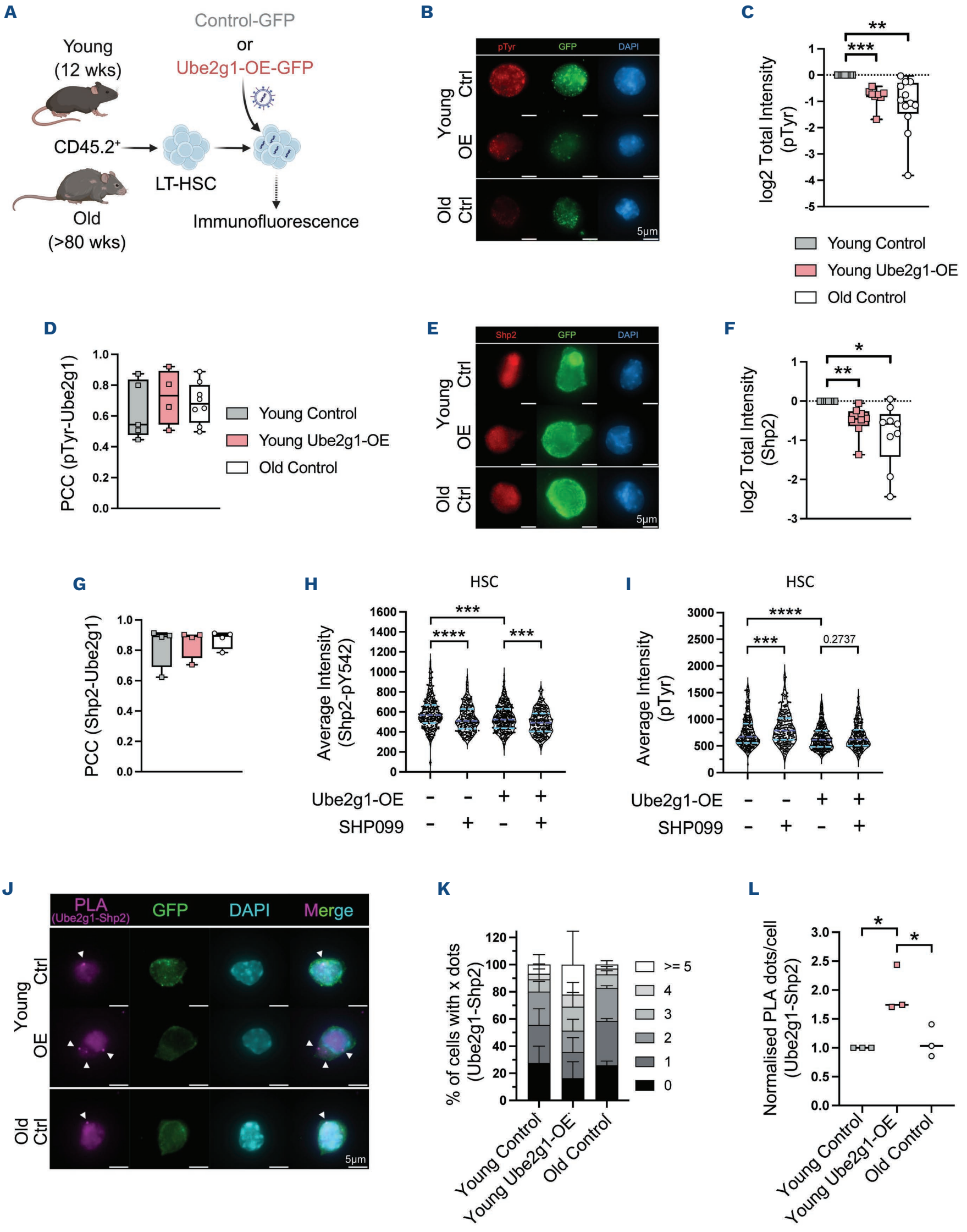


Figure 4. Reduction in global tyrosine phosphorylation and Shp2 phosphatase possibly through direct interaction. (A) Workflow for immunofluorescence preparation of transduced hematopoietic stem cells (HSC) from young (12-16 weeks [wks], wild-type [WT]) and aged (>80 wks, WT) mice. (B) Representative immunofluorescence (IF) images from young and old control and young

Continued on following page.

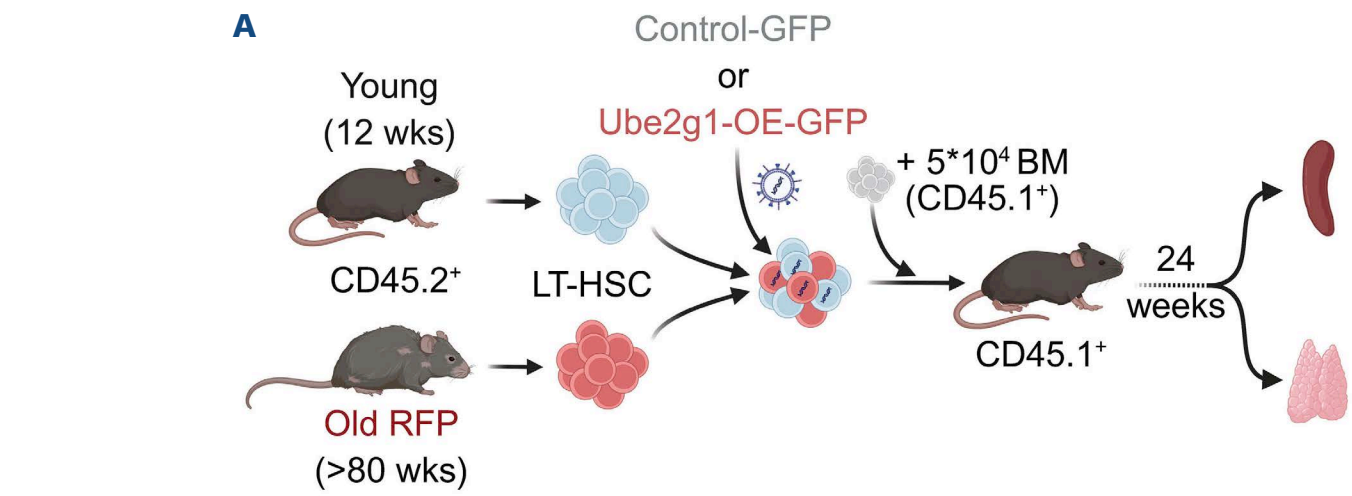
Ube2g1-overexpression (OE) transduced murine HSC stained for global tyrosine phosphorylation (red), GFP (green), and DAPI (blue). Scalebar = 5μm. (C) Relative (log2 transformed) intensity of pTyr in young and old control and young Ube2g1-OE transduced murine HSC. N=8-12, biological repeats equal to an average of 126/123 and 145/158 (young control/overexpression [OE] / old control/OE) cells per replicate. (D) Pearson Correlation Coefficient (PCC) of pTyr and Ube2g1 in young and old control and young Ube2g1-OE transduced murine HSC (N=4-8). (E) Representative IF images from young and old control and young Ube2g1-OE transduced murine HSC stained for Shp2 (red), GFP and DAPI. Scalebar = 5μm. (F) Relative (log2 transformed) intensity of Shp2 in young and old control and young Ube2g1-OE transduced murine HSC. N=7-8, biological repeats equal to an average of 135/157 and 174/166 (young control/OE, old control/OE) cells per replicate. (G) PCC of Shp2 and Ube2g1 in young and old control and young Ube2g1-OE transduced murine HSC (N=3). (H) Average intensity of Shp2-pY542 in young control and Ube2g1-OE HSC either untreated or treated with 100μM SHP099 for 15 minutes. N=246-364 cells from 4 biological repeats. (I) Average intensity of pTyr in young control and Ube2g1-OE HSC either untreated or treated with 100μM SHP099 for 15 minutes. N=245-341 cells from 4 biological repeats. (J) Representative IF images from young and old control and young Ube2g1-OE murine HSC showing PLA signals (Shp2 and Ube2g1) and staining for GFP (transduced cells) and DAPI (nucleus). White arrows indicate PLA interactions (dots). Scalebar = 5μm. (K) Percentage of cells with 0, 1, 2, 3, 4 or ≤ 5 PLA interaction dots. N=3, biological repeats equal to an average of 203/211 and 376 (young control/OE, old control) cells per replicate. (L) PLA signal (Ube2g1-Shp2) per cell normalized to young control. N=3, biological repeats equal to an average of 203/211 and 376 (young control/OE, old control) cells per replicate. Data show individual biological replicates with each replicate as mean ± standard deviation. Data were assessed by a One sample *t* test against a value of 0 for young control (C, D, F, G, L) or a non-parametric Mann-Whitney test (H, I). **P*<0.05, ***P*<0.01, ****P*<0.001, *****P*<0.0001.

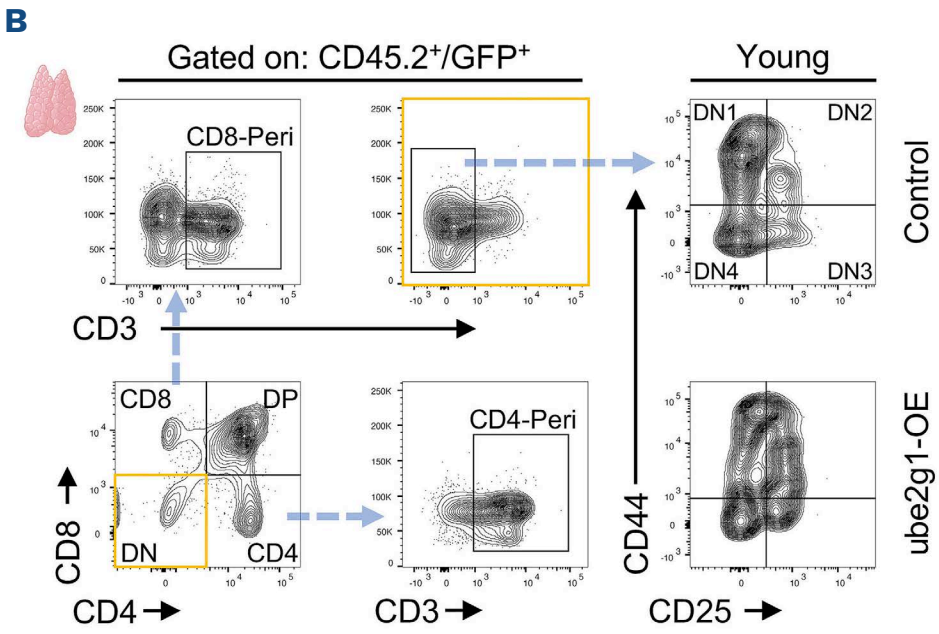
role in stem cell biology.[7,31,37] Ube2g1 belongs to the group of E2 conjugation enzymes. Our data identified elevated levels of Ube2g1 along with K48-Ub in aged murine and human HSC. We demonstrate that increased Ube2g1 levels in murine HSC cause segmental premature aging of the hematopoietic system. The following hallmarks of aging were recapitulated in animals transplanted with young Ube2g1-OE HSC: stem cell exhaustion, immune cell disbalance, myeloid skewing and proteostasis loss. A reduced aging-associated increase in Ube2g1 in aged murine HSC attenuates myeloid skewing by affecting both myeloid and lymphoid differentiation. There is a reduction in naïve T cells concomitant with an increase in exhausted peripheral T cells in response to elevated levels of Ube2g1 in HSC. Elevated levels of Ube2g1 resulted in elevated levels of exhaustion markers like Tim-3 on peripheral T cells. Elevated levels of Tim-3 expression/exhaustion were shown to be linked to myelodysplastic HSC and leukemic stem cells (LSC),[38,39] which might link Ube2g1 to an enhanced clonal selection of HSC. However, we did not observe myelodysplastic syndrome-related morphological or cytological changes driven by Ube2g1-OE HSC up to 24 weeks post transplantation in our recipients, possibly due to insufficient exposure time or lack of additional stressors. Additionally, we found Ube2g1-OE T cells to be less activated compared to controls upon *in vitro* expansion/activation culture, with a decrease in the level of active Shp2 (pY542) and an increase in the level of pTyr, supporting a role for an Ube2g1-OE-Shp2-pTyr axis in T-cell activation. Likely due to the overall low number of T cells within the BM, premature aging was less prominent among BM cells compared to spleen and blood. These data also imply that lymphocytes derived from OE HSC may be less capable of mounting an adequate immune response, which will be an interesting hypothesis to test in future experiments.

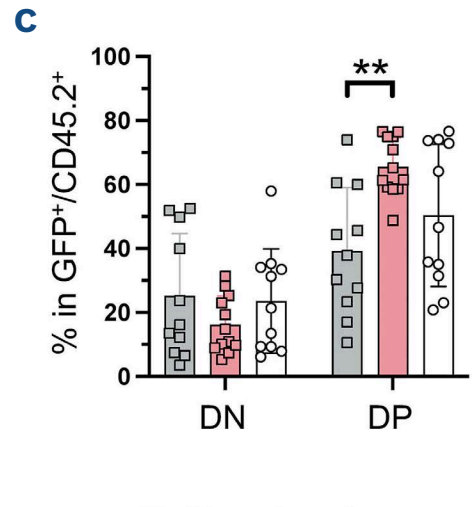
Surprisingly, our data suggest that the ubiquitin-conjugating activity of Ube2g1 is probably not the central underlying mechanisms for conferring the aging-associated phenotypes, while transcriptome analyses identified several E3 ligases (Cbl, Traf6, Fbxw7, Hectd1, Hectd2) as up-regulated in response to Ube2g1-OE. Although the pulldown-data in NIH/3T3 cells did not indicate direct protein-protein interactions with any of these E3 ligases, indirect interactions via shared degradation substrates or subsequent altered phosphorylation signaling remain an alternative mode of interaction. This might imply that distinct levels of Ube2g1 affect the regulation of the general ubiquitin-proteasome system in HSC, which would be consistent with the elevated levels of K48-Ub found in aged murine and human HSC. Whether elevated levels of K48-Ub are mechanistically linked to conferring segmental aging phenotypes remains to be determined.

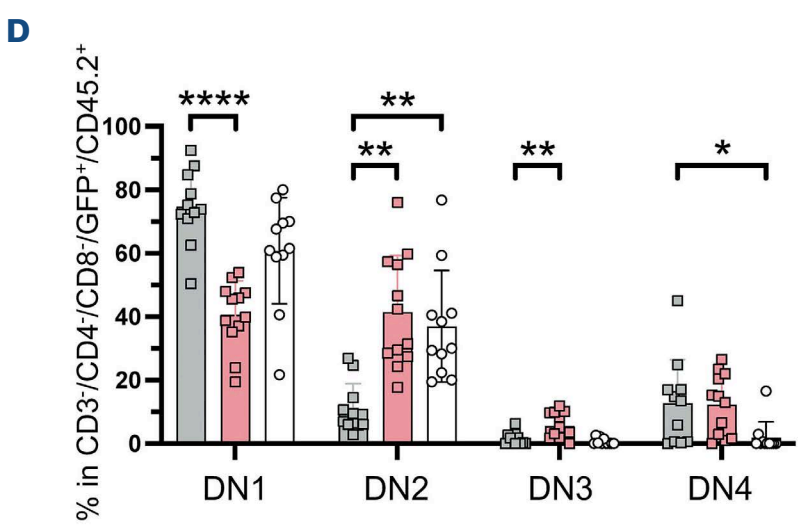
We identified a cluster of heat shock proteins, including Hspa8, as potential Ube2g1 interactors. Notably, the level of Hsf1, a key regulator of the heat shock response and an important regulator of for HSC function,[11] was also reduced in Ube2g1-OE HSC, implying that the proteostasis might also be affected by Ube2g1 in HSC.

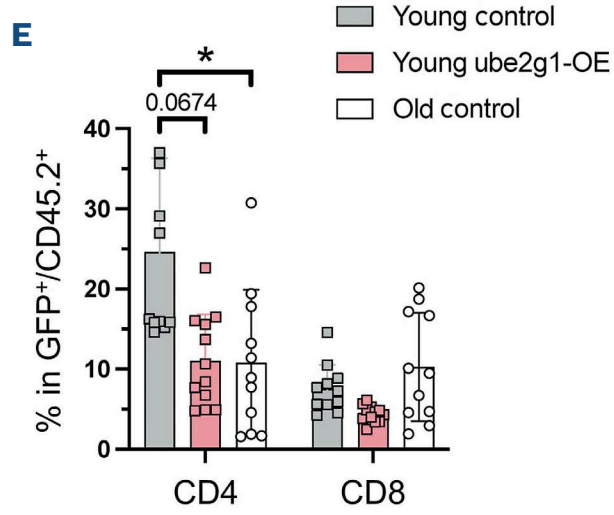
We show here both a reduction in tyrosine phosphorylation and in total levels of Shp2 in aged and Ube2g1-OE HSC. Shp2 is a phosphatase and thus negatively regulates tyrosine phosphorylation residues. Dysfunctional Shp2 signaling is known to play a role in HSC biology and T-cell development.[40,41] Furthermore, impaired tyrosine phosphorylation strongly correlates with dysfunctional T-cell development and T-cell receptor (TCR) signaling due to changes in MAPK/ERK or JAK/STAT signaling pathways downstream of the TCR.[42,43] The observed loss of tyrosine phosphorylation might lead to disrupted initiation and propagation of TCR signaling, essential for T-cell development in hematopoiesis.[44,45] Additionally, loss of tyrosine phosphorylation inactivates kinases like Zap70 and Lck, proven to be vital for thymic T-cell selection.[46,47] Dysregulation of such pathways in aging/response to Ube2g1-OE might contribute to altered T-cell maturation and the more exhausted adaptive immune system. This would initially imply that Shp2 is likely not

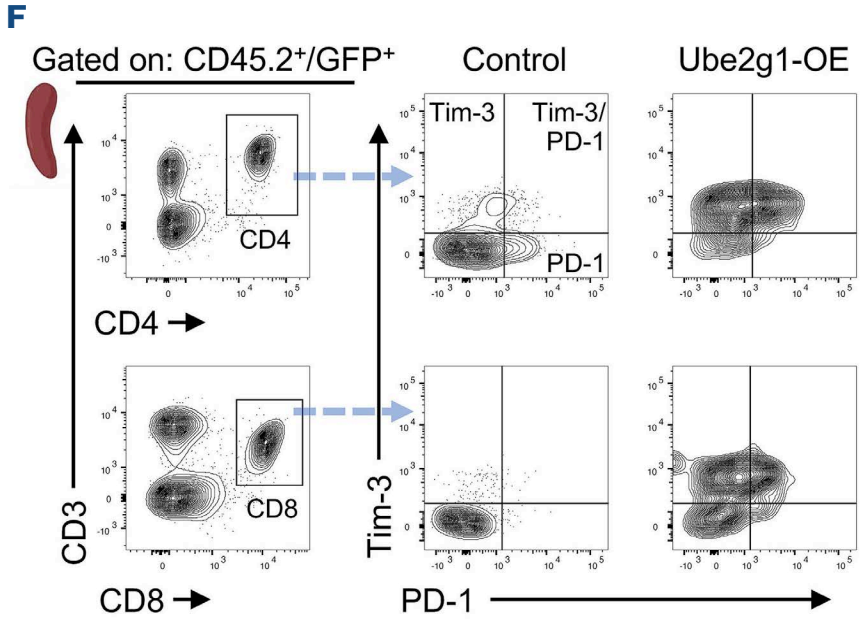


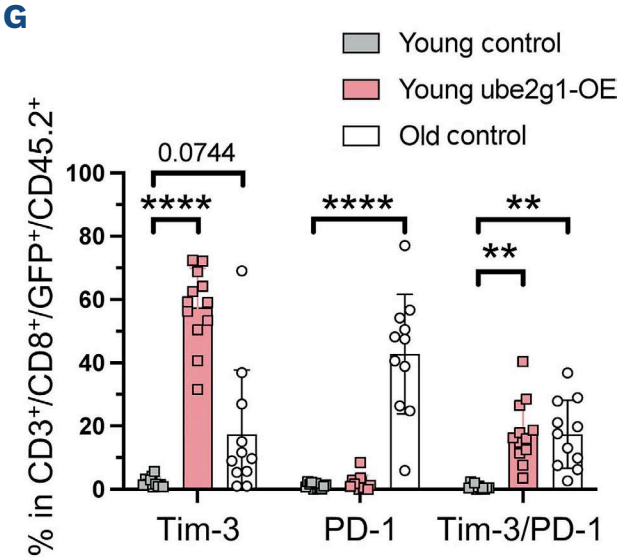












Continued on following page.

Figure 5. Elevated levels of Ube2g1 results in attenuated T-cell development in the thymus and increased exhaustion in released peripheral T cells. (A) Experimental set-up of the competitive transplantation experiment, using sorted hematopoietic stem cells (HSC) from young (12-16 weeks [wks], wild-type [WT]) and aged (>80 wks, AcRFP$^+$) donor mice (CD45.2$^+$). HSC were genetically engineered and transplanted alongside 5 x10^4 CD45.1$^+$ bone marrow (BM) cells into lethally irradiated recipient mice (CD45.1$^+$). (B) Representative flow cytometry plots showing thymocytes gated for young and aged CD4/CD8 double negative (DN) and positive (DP) cells. Single positive CD4 and CD8 cells were gated for CD3. DN cells (yellow box) were gated for CD3-negative and then for CD44/CD25 to identify DN subpopulations DN1-4 (DN1; CD44$^+$CD25$^-$, DN2; CD44$^+$CD25$^+$, DN3; CD44$^-$CD25$^+$, DN4; CD44$^-$CD25$^-$). Indicative DN1-4 gating for young control- and overexpression (OE)-derived thymocytes are depicted. (C) Percentage of donor-derived (GFP$^+$) DN and DP cells in thymus 24 weeks post transplantation (N=11-12). (D) Percentage of donor-derived (GFP$^+$) DN1-4 cells in the thymus 24 weeks post transplantation (N=11-12). (E) Percentage of donor-derived (GFP$^+$) single positive peripheral (CD3$^+$) CD4 and CD8 cells in the thymus 24 weeks post transplantation (N=11-12). (F) Representative flow cytometry plots showing splenocytes gated for young and aged CD4/8-positive T-cell exhaustion markers CD366 (Tim-3) and CD279 (PD-1). Indicative Tim-3/PD-1 gating for young control and OE-derived splenocytes are depicted. (G) Percentage of donor-derived (GFP$^+$) Tim-3 and/or PD-1 exhaustion markers on CD8$^+$ T cells in the spleen 24 weeks post transplantation (N=11-12). Data show individual biological replicates from 2 independent experiment repeats as mean ± standard deviation (SD). Data were assessed by One-Way ANOVA or Kruskal-Wallis test depending on normality (C-E, G). *P<0.05, **P<0.01, ****P<0.0001.

directly linked to the changes in phosphorylation observed. On the other hand, we observed increased levels of active Shp2 (pY542), which is then consistent with a lower overall tyrosine phosphorylation in HSC.

Our proteomic data further identified Shp2 as a potential direct Ube2g1 interactor, which is supported by co-localization and interactions below 40 nm in HSC, linking Ube2g1 to the regulation of tyrosine phosphorylation. While inhibition of Shp2 activity resulted, as expected, in increased levels of phosphorylated proteins in young HSC, it did not affect pTyr levels in Ube2g1-OE HSC. Possibly, Ube2g1 can act as a signaling platform that balances Shp2 signaling and by this means contribute to the level of protein phosphorylation. In such a model, the proper propagation of the signal of Shp2 is impaired if Ube2g1 is disturbed. As we also report a direct interaction of Ube2g1 with Creb3 and Uba52 in HSC, Ube2g1 might form a broader mechanistic/physical protein platform, a hypothesis that will need to be tested in future experiments.

In summary, our findings identify Ube2g1 as a regulator of age-associated changes in HSC biology, particularly affecting T-cell development and exhaustion, but also myeloid differentiation driven by HSC. This likely occurs via mechanisms that involve phosphorylation driven mechanisms, Shp2-mediated pathways, proteostasis and ubiquitin signaling pathways.

Disclosures

No conflicts of interest to disclose.

Contributions

JN is responsible for conceptualization, data curation, formal analysis, investigation, methodology, project administration, software, supervision, visualization, writing the original draft, and reviewing and editing the manuscript; TS is responsible for conceptualization, data curation, investigation, software, and reviewing and editing the manuscript; VS and KS are responsible for conceptualization, investigation, and reviewing and editing the manuscript; AB is responsible for conceptualization, data curation, formal analysis, investigation, and reviewing and editing the manuscript; SW is responsible for data curation, formal analysis, investigation, resources, visualization, and reviewing and editing the manuscript; KE is responsible for conceptualization, investigation, methodology, and reviewing and editing the manuscript; MH and AL are responsible for resources and data curation; MO and HR are responsible for resources, data curation, and reviewing and editing the manuscript; MAM is responsible for conceptualization, data curation, formal analysis, investigation, software, resources, visualization, and reviewing and editing the manuscript; HG is responsible for conceptualization, funding acquisition, methodology, project administration, resources, supervision, writing the original draft, and reviewing and editing the manuscript.

Acknowledgments

We thank the members of the Institute of Molecular Medicine for their valuable comments and discussions. We are also grateful to the Core Facility Cytometry at Ulm University for their support in performing experiments. Special thanks go to the Tierforschungszentrum at Ulm University for their assistance with mouse handling and housing.

Funding

The work was supported by the Deutsche Forschungsgemeinschaft (DFG, German Research Foundation) SFB1074 and SFB1506 Aging@Interfaces (to HG).

Data-sharing statement

The authors confirm that the data supporting the findings of this study are available within the article and its Online Supplementary Appendix. Raw data are available under accession numbers GSE303039 and MSV000098473.

References

1. Laurenti E, Göttgens B. From haematopoietic stem cells to complex differentiation landscapes. Nature. 2018;553(7689):418-426.
2. Pinho S, Frenette PS. Haematopoietic stem cell activity and interactions with the niche. Nat Rev Mol Cell Biol. 2019;20(5):303-320.
3. Geiger H, De Haan G, Carolina Florian M. The ageing haematopoietic stem cell compartment. Nat Rev Immunol. 2013;13(5):376-389.
4. Mejia-Ramirez E, Florian MC. Understanding intrinsic hematopoietic stem cell aging. Haematologica. 2020;105(1):22-37.
5. de Haan G, Lazare SS. Aging of hematopoietic stem cells. Blood. 2018;131(5):479-487.
6. López-Otín C, Blasco MA, Partridge L, Serrano M, Kroemer G. Hallmarks of aging: an expanding universe. Cell. 2023;186(2):243-278.
7. Moran-Crusio K, Reavie LB, Aifantis I. Regulation of hematopoietic stem cell fate by the ubiquitin proteasome system. Trends Immunol. 2012;33(7):357-363.
8. Signer RAJ, Magee JA, Salic A, Morrison SJ. Haematopoietic stem cells require a highly regulated protein synthesis rate. Nature. 2014;509(7498):49-54.
9. Noormohammadi A, Calculli G, Gutierrez-Garcia R, Khodakarami A, Koyuncu S, Vilchez D. Mechanisms of protein homeostasis (proteostasis) maintain stem cell identity in mammalian pluripotent stem cells. Cell Mol Life Sci. 2018;75(2):275-290.
10. Pickart CM, Eddins MJ. Ubiquitin: structures, functions, mechanisms. Biochim Biophys Acta Mol Cell Res. 2004;1695(1-3):55-72.
11. Kruta M, Sunshine MJ, Chua BA, et al. Hsf1 promotes hematopoietic stem cell fitness and proteostasis in response to ex vivo culture stress and aging. Cell Stem Cell. 2021;28(11):1950-1965.e6.
12. Liu B, Zhang X, Zhou Y, et al. USP4 regulates ribosome biogenesis and protein synthesis for hematopoietic stem cell regeneration and leukemia progression. Leukemia. 2024;38(11):2466-2478.
13. Chua BA, Signer RAJ. Hematopoietic stem cell regulation by the proteostasis network. Curr Opin Hematol. 2020;27(4):254-263.
14. Dong Q, Xiu Y, Wang Y, et al. HSF1 is a driver of leukemia stem cell self-renewal in acute myeloid leukemia. Nat Commun. 2022;13(1):1-17.
15. Chua BA, Lennan CJ, Sunshine MJ, et al. Hematopoietic stem cells preferentially traffic misfolded proteins to aggresomes and depend on aggrephagy to maintain protein homeostasis. Cell Stem Cell. 2023;30(4):460-472.
16. Ryu K-S, Choi Y-S, Ko J, et al. Direct characterization of E2-dependent target specificity and processivity using an artificial p27-linker-E2 ubiquitination system. BMP Rep. 2008;41(12):852-857.
17. Stewart MD, Ritterhoff T, Klevit RE, Brzovic PS. E2 enzymes: more than just middle men. Cell Res. 2016;26(4):423-440.
18. Choi YS, Lee YJ, Lee SY, et al. Differential ubiquitin binding by the acidic loops of Ube2g1 and Ube2r1 enzymes distinguishes their Lys-48-ubiquitylation activities. J Biol Chem. 2015;290(4):2251-2263.
19. Lu G, Weng S, Matyskiela M, et al. UBE2G1 governs the destruction of cereblon neomorphic substrates. Elife. 2018:7:e40958.
20. Masuda S, Kurabayashi N, Nunokawa R, et al. TRAF7 determines circadian period through ubiquitination and degradation of DBP. Commun Biol. 2024;7(1):1-12.
21. Qiang J, Yu S, Li J, et al. Single-cell landscape of alternative polyadenylation in human lymphoid hematopoiesis. J Mol Cell Biol. 2024;16(7):1-16.
22. Schuster T, Amoah A, Vollmer A, et al. Quantitative determination of the spatial distribution of components in single cells with CellDetail. Nat Commun. 2024;15(1):1-13.
23. Brown LY, Dong W, Kantor B. An improved protocol for the production of lentiviral vectors. STAR Protoc. 2020;1(3):100152.
24. Hecht M, Rösler R, Wiese S, Johnsson N, Gronemeyer T. An interaction network of the human SEPT9 established by quantitative mass spectrometry. G3 (Bethesda). 2019;9(6):1869-1880.
25. Cox J, Mann M. MaxQuant enables high peptide identification rates, individualized p.p.b.-range mass accuracies and proteome-wide protein quantification. Nat Biotechnol. 2008;26(12):1367-1372.
26. Cox J, Neuhauser N, Michalski A, Scheltema RA, Olsen JV, Mann M. Andromeda: a peptide search engine integrated into the MaxQuant environment. J Proteome Res. 2011;10(4):1794-1805.
27. Florian MC, Klose M, Sacma M, et al. Aging alters the epigenetic asymmetry of HSC division. PLoS Biol. 2018;16(9):1-35.
28. Leins H, Mulaw M, Eiwen K, et al. Aged murine hematopoietic stem cells drive aging-associated immune remodeling. Blood. 2018;132(6):565-576.
29. Eden E, Navon R, Steinfeld I, Lipson D, Yakhini Z. GOrilla: a tool for discovery and visualization of enriched GO terms in ranked gene lists. BMC Bioinformatics. 2009;10(1):1-7.
30. Kustikova O, Fehse B, Modlich U, et al. Clonal dominance of hematopoietic stem cells triggered by retroviral gene marking. Science. 2005;308(5725):1171-1174.
31. Fatima A, Irmak D, Noormohammadi A, et al. The ubiquitin-conjugating enzyme UBE2K determines neurogenic potential through histone H3 in human embryonic stem cells. Commun Biol. 2020;3(1):1-19.
32. Ciechanover A, Kwon YT. Degradation of misfolded proteins in neurodegenerative diseases: therapeutic targets and strategies. Exp Mol Med. 2015;47(3):1-16.
33. David DC, Ollikainen N, Trinidad JC, Cary MP, Burlingame AL, Kenyon C. Widespread protein aggregation as an inherent part of aging in C. elegans. PLoS Biol. 2010;8(8):47-48.
34. Cuanalo-Contreras K, Schulz J, Mukherjee A, Park K-W, Armijo E, Soto C. Extensive accumulation of misfolded protein aggregates during natural aging and senescence. Front Aging Neurosci. 2023;14(11):1-15.
35. Guidi N, Marka G, Sakk V, Zheng Y, Florian MC, Geiger H. An aged bone marrow niche restrains rejuvenated hematopoietic stem cells. Stem Cells. 2021;39(8):1101-1106.
36. Nikolich-Žugich J. Aging of the T cell compartment in mice and humans: from no naive expectations to foggy memories. J Immunol. 2014;193(6):2622-2629.
37. Zhan Q, Wang J, Zhang H, Zhang L. E3 ubiquitin ligase on the biological properties of hematopoietic stem cell. J Mol Med. 2023;101(5):543-556.
38. Tao J-L, Li L-J, Fu R, et al. Elevated TIM3+ hematopoietic stem cells in untreated myelodysplastic syndrome displayed aberrant differentiation, overproliferation and decreased apoptosis. Leuk Res. 2014;38(6):714-721.
39. Kikushige Y, Shima T, Takayanagi SI, et al. TIM-3 is a promising target to selectively kill acute myeloid leukemia stem cells. Cell

Stem Cell. 2010;7(6):708-717.
40. Zhu HH, Ji K, Alderson N, et al. Kit-Shp2-Kit signaling acts to maintain a functional hematopoietic stem and progenitor cell pool. Blood. 2011;117(20):5350-5361.
41. Solman M, Blokzijl-Franke S, Piques F, et al. Inflammatory response in hematopoietic stem and progenitor cells triggered by activating SHP2 mutations evokes blood defects. Elife. 2022;11(e):73040.
42. Liu X, Qu C-K. Protein tyrosine phosphatase SHP-2 (PTPN11) in hematopoiesis and leukemogenesis. J Signal Transduct. 2011:2011:195239.
43. Williams MJ, Wang X, Bastos HP, et al. Maintenance of hematopoietic stem cells by tyrosine-unphosphorylated STAT5 and JAK inhibition. Blood Adv. 2025;9(2):291-309.
44. Shah K, Al-Haidari A, Sun J, Kazi JU. T cell receptor (TCR) signaling in health and disease. Signal Transduct Target Ther. 2021;6(1):1-26.
45. Stanford SM, Rapini N, Bottini N. Regulation of TCR signalling by tyrosine phosphatases: from immune homeostasis to autoimmunity. Immunology. 2012;137(1):1-19.
46. Castro-Sanchez P, Teagle AR, Prade S, Zamoyska R. Modulation of TCR signaling by tyrosine phosphatases: from autoimmunity to immunotherapy. Front Cell Dev Biol. 2020:8:608747.
47. Hwang JR, Byeon Y, Kim D, Park SG. Recent insights of T cell receptor-mediated signaling pathways for T cell activation and development. Exp Mol Med. 2020;52(5):750-761.